Geophysical Research Letters

RESEARCH LETTER
10.1029/2020GL091767

Asymmetric Magnetic Anomalies Over Young Impact Craters on Mercury

V. Galluzzi[1], J. S. Oliveira[2,3], J. Wright[4], D. A. Rothery[4], and L. L. Hood[5]

[1]Istituto di Astrofisica e Planetologia Spaziali, Istituto Nazionale di Astrofisica, Rome, Italy, [2]Science and Operations Department, Directorate of Science, European Space Research and Technology Centre, European Space Agency, Noordwijk, Netherlands, [3]Space Magnetism Area, Payloads & Space Sciences Department, Instituto Nacional de TØcnica Aeroespacial, Torrejón de Ardoz, Spain, [4]School of Physical Sciences, The Open University, Milton Keynes, UK, [5]Lunar and Planetary Laboratory, University of Arizona, Tucson, AZ, USA

Key Points:

- Stieglitz and Rustaveli are two young impact craters on Mercury associated with overlapping crustal magnetic anomalies
- The magnetic anomalies are asymmetrical with respect to each crater's center and correlate well with the location of impact melt
- The impact melt located downrange contains impactor magnetic-carriers that recorded the magnetic field of Mercury at the time of quenching

Supporting Information:

Supporting Information S1

Correspondence to:
V. Galluzzi,
valentina.galluzzi@inaf.it

Citation:
Galluzzi, V., Oliveira, J. S., Wright, J., Rothery, D. A., & Hood, L. L. (2021). Asymmetric magnetic anomalies over young impact craters on Mercury. Geophysical Research Letters, 48, e2020GL091767. https://doi.org/10.1029/2020GL091767

Received 19 NOV 2020
Accepted 25 JAN 2021

Abstract Mercury's crustal magnetic field map includes anomalies that are related to impact craters. Mercury's surface has a low iron abundance, but it is likely that some impactors brought magnetic carriers able to register the planet's magnetic field that was present during impact. Anomalies associated with the relatively young Rustaveli and Stieglitz craters are asymmetric with respect to the crater center. We analyze the location of the magnetic anomalies and the impact crater morphologies to understand whether there is any correlation. We investigate the geological framework of these two craters to constrain the overall impact dynamics. In both cases, magnetic anomalies correlate well with the location of impact melt and the inferred impact direction. Both impact angles were probably 40° 45°, with preferential distribution of the melt downrange. Inversion dipoles suggest that the impact melt located downrange encompasses some magnetized material, which is hence likely responsible for the detected magnetic anomalies.

Plain Language Summary We observe strong crustal magnetic field imprints near two recent craters on Mercury. We know that the crust of rocky planets may include magnetic elements like iron that can record the local magnetic field under certain circumstances. However, Mercury's crust is known to be remarkably poor in iron. In this study, we want to find out whether these observed magnetic imprints near craters happened by chance or if it can be explained by the impactors bringing iron to Mercury's surface. We make a joint-study of two different scientific areas: Geology and geophysics. Via the geological study, we found an uneven distribution of impact melt, which is material flung out of the crater in molten form during the impact that made the crater. Via the geophysical study, we found evidence that magnetized material correlates with the position of those pools that are found in the downrange direction of the impact. In conclusion, this study supports the hypothesis that iron was brought on Mercury by the impactors.

1. Introduction

The low-altitude campaign (<120 km) of the NASA MErcury Surface, Space ENvironment, GEochemistry, and Ranging (MESSENGER) mission was fundamental for detecting magnetic field signatures of crustal origin on Mercury (Johnson et al., 2015). However, constraints on the orbit imposed by Mercury's hostile environment allowed these measurements only in a short latitudinal range, between 35°N and 75°N. Maps of the crustal magnetic field at 40 km altitude (Hood, 2016; Hood et al., 2018) show that most of the surface is scarcely magnetized, but with some magnetic anomalies heterogeneously distributed over the surface of the planet. These anomalies do not seem to be related to any specific geological features, except for a few cases where the anomalies are found to be related to basins or craters (Hood et al., 2018; Oliveira et al., 2019a). For example, the strongest signal of the Hermean crustal magnetic field is detected over the Caloris basin, and has an intensity of about 9.5 nT at 40 km altitude (Hood, 2016), which is comparable to, or somewhat larger than the strongest lunar crustal anomaly intensities (e.g., Richmond & Hood, 2008).

The composition of the magnetic anomalies sources are poorly understood, particularly given that spectroscopic observations have revealed that Mercury's surface is poor in iron (Izenberg et al., 2014; Weider et al., 2014), which would be the best magnetic carrier to record magnetic fields. Understanding their origin

is important, because a thermoremanently magnetized body probably holds information about the past core field, which allows understanding of the dynamo evolution, and consequently Mercury's history.

For the Moon, Wieczorek et al. (2012) proposed that impactors could deliver magnetic carriers to the surface, and that in the presence of a core magnetic field this material would become magnetized. This hypothesis was recently suggested for Mercury as well (Hood et al., 2018). This process would result in some craters that are related to anomalies and others that are not, depending on the impactor composition. The eventual distribution of the impactor material depends on several variables: velocity, angle and composition of the impactor, and composition of the surface (Wieczorek et al., 2012). Most of Mercury's original crust has been volcanically resurfaced (e.g., Thomas & Rothery, 2019). Most iron-enriched impact melt and ejecta from basins such as Caloris are likely to lie beneath these flows, rather than at the surface. General correlative studies of magnetic field intensity versus surface composition and geology may therefore not be successful in positively identifying magnetic anomaly source materials.

Here, we test the impactor delivery hypothesis by investigating some anomalies that are related, but asymmetrical, with respect to young craters. Inferring the craters impact geometries from geological indicators will help understanding whether the off-centered anomalies are related to the impactor-delivered materials or not.

1.1. Geological Context

The area between 35°N and 75°N, where crustal magnetic field signatures could be detected, is largely covered by a series of four quadrangle geological maps at 1:3M-scale (Galluzzi et al., 2016; Guzzetta et al., 2017; Mancinelli et al., 2016; Wright et al., 2019) that Hood et al. (2018) used to locate regions of interest where magnetic anomalies overlap geological features. The strongest magnetic anomalies are found over the Caloris impact region, both inside Caloris Planitia and over the circum-Caloris smooth plains. The area 90°E 270°E is largely biased by Caloris-based anomalies, but the opposite longitudes offer the chance to locate some magnetic anomalies that are correlated with isolated features far from this large basin (Figure 1). The most significant ones are located at Vyasa crater (275°E; 50°N), the B31 basin (3°E; 36°N; Orgel et al., 2020), the Northern Rise (30°E; 68°N; Zuber et al., 2012), Rustaveli crater (82°E; 52°N), and Stieglitz crater (67°E; 73°N) (Hood et al., 2018; Figure 1). Vyasa and the B31 basin are very old impact sites, degraded and overlapped by other craters, hence the magnetic anomalies origins are difficult to interpret. On the other hand, the latter three sites are all located within the young Borealis Planitia characterized by smooth plains, the youngest extensive plains unit on Mercury. These are widespread effusive volcanic plains thought to be as old as 3.7 Ga (Ostrach et al., 2015) and not younger than 3.5 Ga (Byrne et al., 2016). There is no clear evidence on Mercury that effusive volcanism alone brought magnetic carriers to the upper crust. In fact, Borealis Planitia does not show widespread magnetic anomalies (Hood et al., 2018).

Stieglitz and Rustaveli craters, located within Borealis Planitia and away from the localized Northern Rise magnetic anomaly, represent an interesting case study for understanding whether some impactors played a role as suppliers of magnetic carriers to Mercury's crust. Differently from all other features corresponding to the magnetic anomalies listed above, these two young and fresh craters, which still maintain fresh morphologies and are younger than nearby volcanic plains, offer the chance to study their impact dynamics and to relate these to the relative location of their off-center magnetic anomalies. These are the only two craters that permit such a study within the available crustal magnetic field map.

2. Geological Results

We used the MESSENGER Mercury Dual Imaging System (MDIS; Hawkins et al., 2007) basemap datasets and the available Digital Terrain Models (DTM, Stark et al., 2017; Becker et al., 2016) to map the geomorphology of Stieglitz and Rustaveli craters by using the mapping methods described in Galluzzi (2019). For complete information on the datasets and methods used for this analysis see the supporting information (Text S1).

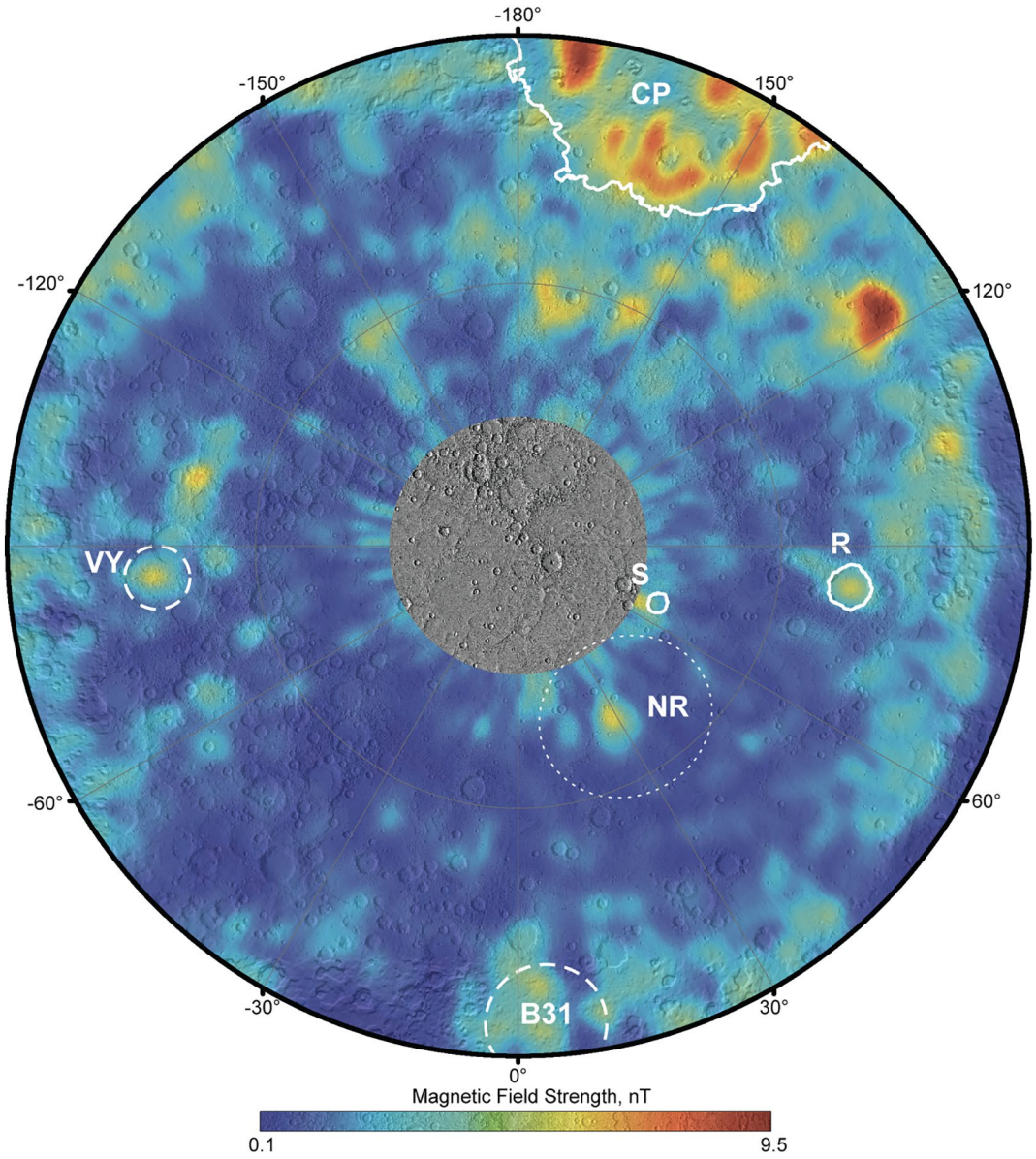

Figure 1. Magnetic field intensity at 40 km altitude (resolution of 1°, Hood et al., 2018) superposed on a MLA shaded relief basemap in stereographic north pole projection (from 35°N to 90°N). Major anomalies cited in the text are labeled with letters and the associated feature extent is indicated by outlines. Caloris Planitia (CP), Rustaveli crater (R), and Stieglitz crater (S) are shown with solid white outlines. The ancient basins Vyasa (VY) and B31 basin (B31) are indicated by dashed outlines. The approximate extent of the Northern Rise (NR) is shown with a white dotted outline. MLA, Mercury Laser Altimeter.

2.1. Stieglitz Crater

Stieglitz crater is a mature-complex crater (see morphologic crater classification of Baker et al., 2011; for details) located in Borealis Planitia, just outside the north-eastern limit of the Northern Rise (67.63°E; 72.53°N). Stieglitz has a roughly circular outline with a slight tendency toward polygonality and has a U-shaped central peak with bilateral symmetry (Figure 2a). It is the youngest crater of its size in its surrounding area (Figure 2a) and belongs to degradation class c4 in the 5-class system by Kinczyk et al. (2020) and would be classified as a C3 in the 3-class system used by Galluzzi et al. (2016) (note our convention of using c for the 5-class system and C for the 3-class system, where both systems use higher numbers to indicate less degradation). This and its stratigraphic position suggest a Mansurian age (e.g., Wright

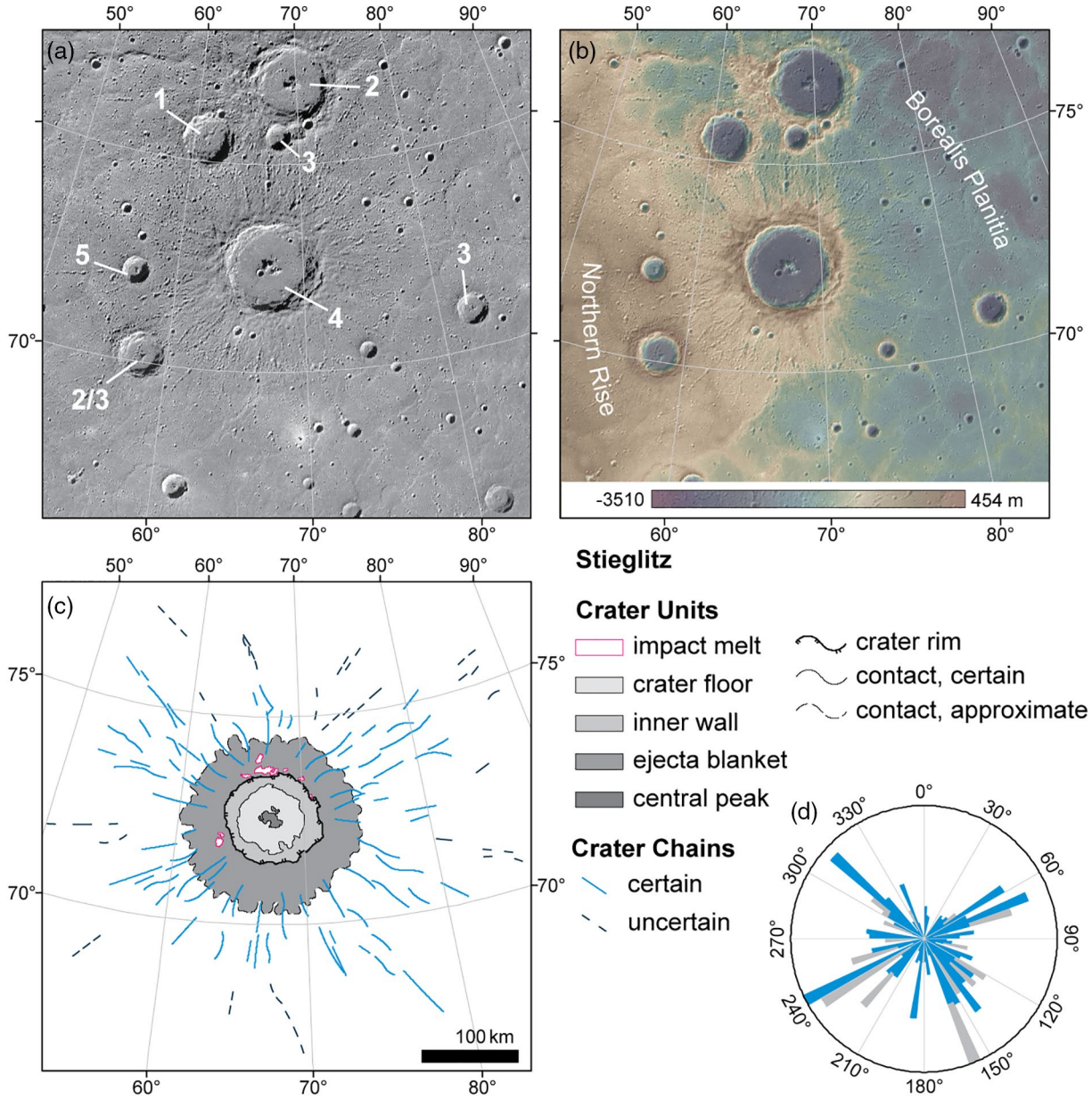

Figure 2. Stieglitz crater in stereographic projection centered on the crater center (67.63°E; 72.53°N): (a) relative age of Stieglitz and the surrounding craters from the oldest (1) to the youngest (5) on the High-Incidence from East basemap at 166 m/pixel; (b) MLA north-polar DTM; (c) simplified geological map showing the trend of certain and uncertain secondary crater chains related to the Stieglitz impact; (d) rose diagram analysis of crater chains showing the start and end azimuth of chains indicated by the blue and gray bins, respectively, obtained with Polar Plots tool by Jenness (2014). DTM, Digital Terrain Model; MLA, Mercury Laser Altimeter.

et al., 2019). Its diameter is ~95 km but increases up to ~105 km in the NW SE direction apparently mostly because of crater-wall collapses associated with terrace formation. The Mercury Laser Altimeter (MLA; Cavanaugh et al., 2007) north polar DTM reveals that the rim is slightly higher in the arc tracing the SW rim than on the opposite side (Figure 2b).

Overall, a broad degree of radial symmetry can be observed in the continuous ejecta blanket that extends up to ~ one crater radius from most of the rim crest, but slightly farther in the SW (Figure 2c). The crater central peak is at the center of the floor and its U-shape opens toward the SW. A few isolated central peak outliers are located to the NE of the main peak (Figure 2c). The continuous ejecta includes smooth patches of the kind generally interpreted as melt pools (e.g., Chapman et al., 2018; Wright et al., 2019), which is

supported by analogy with lunar examples (e.g., Hawke & Head, 1977). At Stieglitz, these are a few kilometers across and mostly clustered on the northern part of the blanket close outside the crater rim. Some less extensive pools are found WSW of the crater rim (Figure 2c).

A more pronounced asymmetry is observed by analyzing the secondary crater chains directly associated with the Stieglitz impact (Figures 2c and 2d). These extend further in the NW-SE and NE-SW directions, while there is a discernable deficiency of chains at the NNE of the crater, overall showing an axial symmetry in the NNE-SSW direction.

2.2. Rustaveli Basin

Rustaveli (82.74°E; 52.41°N, Figure 3a) is a peak-ring basin superposing the smooth plains of Borealis Planitia in the northeast of Mercury's Hokusai quadrangle. Wright et al. (2019) mapped Rustaveli as degradation class c4 in the 5-class system and C3 in the 3-class system. This and its stratigraphic position suggest a Mansurian age (e.g., Wright et al., 2019), as for Stieglitz crater. The crater rim is symmetrical, but slightly higher in its southeastern arc (Figure 3b), and also somewhat polygonal. A radially textured ejecta blanket (mapped in the same way as for Stieglitz) extends about one crater diameter from the rim at all azimuths (Figure 3c). Numerous patches of smooth plains are perched in the ejecta proximal to Rustaveli's southeastern rim (Figure 3c). These smooth patches are probably ponded impact melt that was ejected from the crater cavity during excavation (Wright et al., 2019). Much more extensive smooth plains extend across the whole of Rustaveli's interior, and those materials are sufficiently thick that only the tops of the basin's peak-ring elements are apparent. The volume necessary to achieve this suggests that at least some of the smooth material within Rustaveli was emplaced by postimpact volcanism, overlying any melt produced by the impact. The exposed peak-ring appears somewhat elliptical, with its long-axis oriented east west (Wright et al., 2016). Our map of secondary crater chains shows a deficiency of chains between W and NW (Figures 3c and 3d). Figure 3c also shows a slight deficiency of chains in the southern part, in the region of a preexisting 50 km diameter crater. We have no explanation of how a preexisting craters could affect secondary impacts (or secondary crater retention) over such a wide area, so this may be no more than random variation. Because chains are not all exactly radial this local deficiency is not so apparent in Figure 3d, which records direction rather than location.

3. Observable Asymmetries and Impact Dynamics

3.1. Stieglitz Crater Impact Analysis

We consider two possible impact scenarios for Stieglitz fully described in Text S2.

The first one considers the crater's subtle asymmetries as: (a) the deficiency of chains radiating toward the NNE (Figure 2d); (b) the NNE-SSW orientation of the symmetry axis of the U-shaped peak (Figure 2a); (c) the highest observable rim topography at S (Figure 2b); (d) the orientation of the symmetry axis of the continuous ejecta blanket in the NNE-SSW direction (Figure 2c). Instead, the second scenario considers: (a) a wider rim arc toward the N (Figure 2b); (b) the location of most melt pools to the N (Figure 2c); the location of the deepest secondary crater chain to the N (Figure S1a, cf. Figure 2b); the central peak outliers just north of the central peak (Figure 2c).

By comparison with previous studies and simulations on oblique impacts (Ekholm & Melosh, 2001; Elbeshausen et al., 2009; Gault & Wedekind, 1978; Schultz, 1992; Kenkmann et al., 2014; Neish et al., 2014; Pierazzo & Melosh, 2000) the first scenario results in a probable impactor trajectory from NNE to SSW and impact angle range of 40° 50° (Figure S1a, case 1), while the second one results in a probable impactor trajectory from S to N and impact angle range of 40° 45° (Figure S1a, case 2). The latter scenario is better constrained than the first one since it takes into account the preexisting topography (Text S2).